A Decentralized Dynamic Relaying-Based Framework for Enhancing LoRa Networks Performance

Hamza Haif, *Graduate Student Member, IEEE*, Abdelali Arous, *Graduate Student Member, IEEE*, and Hüseyin Arslan, *Fellow, IEEE*

***Abstract*—Long-Range (LoRa) technology holds tremendous potential for regulating and coordinating communication among Internet of Things (IoT) devices due to its low-power consumption and cost-effectiveness. However, LoRa faces significant obstacles, such as reduction in coverage area, a high packet drop ratio (PDR), and an increased likelihood of collisions, all of which result in substandard data rates. In this article, we present a novel approach that employs a relaying node capable of allocating resources dynamically based on signal parameters. In particular, the geometric placement of the relay node is determined by a genetic algorithm that maximizes signal-to-noise ratio (SNR) and signal-to-interference ratio (SIR) success probabilities. Using equal-area-based (EAB) spreading factor (SF) distance allocation scheme, the coverage area is sliced into distinct regions in order to derive the success probabilities for different communication stages. Furthermore, we present a frequency channel shuffling algorithm to prevent collisions between end devices (EDs) without increasing the complexity of the relaying nodes. Through extensive simulations, we demonstrate that our proposed scheme effectively expands the coverage area, conserves transmission resources, and enhances the system's throughput. Specifically, our approach extends the range by up to 40%, increases the throughput by up to 50% compared to conventional methods, and achieves a 40% increase in success probability. To validate the practicality of our approach, we implement our algorithm in an active LoRa network utilizing an ESP32 LoRa SX1276 module, showcasing its compatibility in real-world scenarios.**

***Index Terms*—Genetic algorithm (GA), Long-Range (LoRa), LoRaWAN, relays, scalability, spreading factor (SF), Time on Air (ToA).**

I. Introduction

LOW-POWER wide-area network (LPWAN) architectures have emerged as a promising technologies to facilitate Long-Range (LoRa) communication amongst low-bandwidth Internet of Things (IoT) devices. LPWANs are specifically designed to minimize the overall system cost while enabling seamless connectivity among IoT sensors [1]. As the vision for sixth-generation (6G) wireless networks emphasizes key attributes, such as mass connectivity, energy efficiency, and network scalability [2], the development of network paradigms capable of addressing these demands is of critical importance. Therefore, establishing infrastructures that can support large-scale deployments of IoT devices in an energy-efficient and scalable manner represents a significant research priority.

To meet the stringent requirements of LPWANs, LoRa technology emerges as the most frequently adopted solution among a variety of challengers. Its inherent simplicity, resilience, and compatibility with industrial, scientific, and medical (ISM) bands contribute to its pervasive adoption [3], [4]. LoRa employs a star-of-stars topology to link the distributed end devices (EDs) and the gateway (GW). Notably, the EDs initiate transmission by sending an uplink (UL) signal to the GW using a grant-free ALOHA scheme [5]. Subsequently, the GW forwards these frames to the application server through the network. To ensure successful reception of these UL transmissions, the GW sends an acknowledgment signal back to the ED [6]. Various parameters and factors influence the communication process at every phase, including transmission initiation, signal propagation, environmental influences, and reception followed by deciphering of the transmitted frame. The transmission power (TxPower), coding rate (CR), frequency channels (FCs), and most importantly the use of spreading factor (SF) are crucial factors. More precisely, their importance lies in the following.

1) *SF and Time on Air (ToA):* The SF determines the number of bits per symbol, discernible through either frequency shifts or temporal discontinuities [7]. Higher SFs result in prolonged symbol duration and expanded communication ranges, at the expense of diminished data rates and increased collisions probabilities [8]. Conversely, ToA signifies the elapsed time from the start of a LoRa frame to the receipt of the last symbol, influenced by various factors, such as SF, CR, and bandwidth (Bw) [9]. ToA is regulated by regional institutions, mandating efficient utilization of the allocated time for successful transmission of data payloads [10].
2) *Communication Initiation and Range:* LoRa devices typically adopt default transmission parameters (TxParams) during the initial connection with the GW [6]. Within close proximity to the GW, these default settings suffice successful communication. However, for EDs positioned at considerable distances, those default parameters may prove inadequate. In such cases, the ED needs to

Manuscript received 25 December 2023; revised 2 March 2024; accepted 15 March 2024. Date of publication 20 March 2024; date of current version 7 June 2024. *(Corresponding author: Hamza Haif.)*

The authors are with the Department of Electrical and Electronics Engineering, Istanbul Medipol University, 34810 Istanbul, Turkey (e-mail: hamza.haif@std.medipol.edu.tr; abdelali.arous@std.medipol.edu.tr; huseyinarslan@medipol.edu.tr).

Digital Object Identifier 10.1109/JIOT.2024.3379568

gradually adapt its TxParams, primarily the SF, to an optimal value resulting in an inefficient resource utilization, elevated packet drop ratio (PDR), and increased collision probabilities. Despite the potential of achieving communication ranges of up to 10 km in line-of-sight scenarios, LoRa suffers from a substantial range limitations when sensors are located outside of the GW's coverage area or within wireless unfriendly zones (WUZs) [11], [12]. Consequently, reliable transmission distances are confined to a mere 200–600 m [13].

A. Motivation

The feasibility, practicality, and real-world implementation of the previous solutions remain challenging. Primarily due to constraints in resources, transmission channels, and compatibility with existing standards and deployed networks. Consequently, it becomes evident that any proposed solution must not only improve performance and mitigate existing issues but also seamlessly integrate with current networks and adhere to regulations. In this context, this study introduces an adaptive decentralized relaying mechanism for LoRa systems, leveraging the concept of network smart repeaters [14]. This mechanism specifically addresses the inherent constraints of LoRa networks, particularly those related to communication range, resource allocation, and transmission efficiency while ensuring compatibility with LoRaWAN standards and regional regulations.

B. Contributions

The proposed relaying process involves a device that is indiscernible to the network, concurrently emulates itself as both a GW for sensor nodes and an ED for the primary GW. A geometrically efficient positioning of the relay node is determined through a signal-to-noise ratio (SNR) and signal-to-interference ratio (SIR) maximization process using a genetic algorithm (GA) to explore optimal solutions within network constraints. Then, the smart relay effectively categorizes EDs into three groups based on received signal characteristics, enabling tailored adaptive relaying operations. The main contributions of this work are summarized as follows.

1) *Relay Placement:* A novel positioning algorithm which maximizes SNR and SIR levels while optimizing success probability within each SF region is developed. The coverage area is divided into SF-specific discs using the equal-area-based (EAB) method. Then, we develop a stochastic geometric model reflecting the success probability variations based on distance, SF value, received signal strength indicator (RSSI) threshold, and SF per SIR orthogonality conditions.
2) *Adaptive Relaying Mechanism:* We propose a dynamic forwarding technique that categorizes EDs based on RSSI, SF, and FC extraction, and a predetermined lookup table into three categories.
   a) *Reachable EDs:* Devices which communicate directly and reliably with the GW. The relay does not interfere with their communication to save the resources.
   b) *Unreachable Sensors:* Those devices cannot reach the GW whatever their TxParams are, they benefit from relay signal amplification while locking them into the same SF to optimize the data rate.
   c) *Adjustable EDs:* These devices fall within the GW coverage area, but their TxParams must be adjusted to enable direct communication. Their TxParams are optimized by the relay for direct GW communication, managed through adaptive data rate (ADR) MAC commands.
3) *Success Probability:* The success probabilities of the system's various communication links are analyzed. Specifically, we investigate the communication probabilities between the relay–GW, relay–adjustable/unreachable EDs, and the overall system, to optimize the network's throughput. Likewise, an affordable FC shuffling algorithm is adopted to address the issue of collisions that may occur when identical SF are transmitted simultaneously on the same FC.
4) *Performance Evaluation and Validation:* A profound analysis of the proposed relay system is conducted, considering critical performance indicators. Consequently, extensive simulations and real-world testing validate the relay system's performance, covering positioning algorithm convergence, success probabilities, ToA and power savings, and practical functionality using USRP E310 and SX1276 LoRa modules.

The remainder of this article is organized as follows. Section II provides a comprehensive review of relevant literature. In Sections III and IV, we present our novel algorithm for relay placement and describe the underlying system model. Then, the adaptive relaying scheme is elaborated upon along with the FCs shuffling algorithm. Section V conducts a thorough analysis of the proposed relaying mechanism. Section VI then presents the simulation and experimental results for validation. Finally, Section VII concludes this article.

II. Related Works

Several approaches have been proposed in the literature to enhance, adapt, and compensate the faults and shortcomings of LoRa networks. These methods generally fall into two major categories.

A. Signal Enhancement

Those methods mainly focus on increasing the data rates, SNR-SIR levels and decreasing the collision probabilities. A common approach involves using relays to amplify weaker signals. However, these relays typically amplify all signals indiscriminately, which can lead to power constraints and interference issues within the unlicensed bands [15]. Addressing these concerns, an optimization solution is suggested in [16], where a two-hop amplify-and-forward relaying LoRa network as the GW allocates optimal SF and power values to maximize data rates based of the feedback of the

relaying nodes. Additionally, the LoRa alliance proposes a system relaying mechanism [17], which activates relays via wake-on-radio signals from EDs, thereby modifying both UL and downlink (DL) frames. Alternatively, deploying more GWs in the network is a primitive solution, since in addition to its high cost and the requirement for Internet connectivity, a single GW can accommodate a large number of nodes if an appropriate transmission scheme is employed. Building upon this concept, [18] presents a comprehensive mathematical model that adjusts the distance ring exponential stations generator in which intermediate GWs are distributed in rings based on the Fibonacci distance propagation model, allowing efficient packet forwarding to the primary GW. To coordinate transmissions effectively, [19] proposes a synchronization scheme wherein a central entity encodes time-slot assignments using a probabilistic data structure. Furthermore, a two-step lightweight scheduling approach is proposed in [20] to improve scalability and reliability, by dynamically identifying the allowed TxPowers and SFs on each channel.

B. Multihop Networks

Mesh topologies are based on multiple central retransmission nodes to extend range and reroute signals if direct links encounter unfavorable channel conditions. Mesh configurations have been extensively studied due to their ability to interconnect EDs transmissions, providing scalability and resilience to packet loss by routing signals through the most secure and reliable links [21], [22], [23], [24], [25], [26], [27]. A technique proposed by [25] partitions nodes into high and low SF groups, with the GWs and relays selecting clusters using the naive Bayes algorithm to achieve fairness and high data rate in multihop LoRa networks. To avoid collisions caused by mesh topologies, a novel LoRaHop protocol [26] extends LoRaWAN specifications by forming a mesh network that enables concurrent transmissions to relay UL and DL packets without collision, allowing any node to transmit to the GW without interference using coordination between different nodes. To improve the packet delivery success ratio (PDSR), [27] proposes an implicit overhearing node-based multihop communication (IOMC) scheme which chooses relaying nodes with low SF to perform overhearing and forwarding while adhering to duty cycle constraint. Similarly, A scalable relay control scheme in [28] employs GAs to maximize the coverage probability while jointly minimizing ED's SF and adhering to duty cycle regulations. However, despite their advantages, these architectures face challenges. They often conflict with existing LoRaWAN regulations, as they require EDs to remain continuously active for signal reception and forwarding, draining the sensors' power and consuming their ToA allocation. Additionally, mesh topologies pose security concerns since sensor cryptography keys are shared among multiple nodes forming the routing path [29]. Furthermore, concurrent transmissions and multihop techniques may not adequately account for the propagation environment, resulting in constraints on time window synchronizations and alignments, particularly as the number of EDs increases. Moreover, selectively allocating low SFs to EDs to increase data rates may lead to high collision probabilities, impacting overall system performance negatively, especially when multiple sensors share these resources.

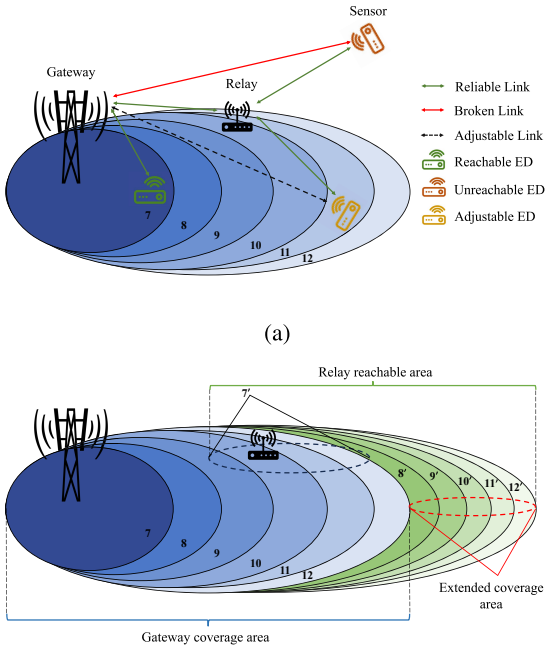

Fig. 1. System model. (a) ED's classification based on communication link. (b) Coverage area as seen per relay.

TABLE I
NOTATIONS AND MATHEMATICAL SYMBOLS

Notation	*Definition*
ED, $\mathcal{C}$, N	*Set of ED, coverage area, number of EDs.*
λ	*EDs distribution intensity.*
SF, CR	*Set of spreading factors, coding rate.*
Bw, **FC**	*Bandwidth, set of frequency channels.*
$\mathrm{R}_{\mathcal{SF}}$, $\mathrm{ToA}_{\mathcal{SF}}$, $\alpha_{\mathcal{SF}}$	*Data rate, ToA and duty cycle for $\mathcal{SF}$.*
P_i, P_r	*TxPower of $\mathcal{ED}_i$ and relay.*
$\mathrm{d}_{i,g}$	*Euclidean distance between $\mathcal{ED}_i$ and GW.*
$\lvert h_{i,g}\rvert^2$	*Channel gain between $\mathcal{ED}_i$ and GW.*
$l(d)$	*PL attenuation at distance d*
η, σ^2	*PL exponent, noise variance.*
$\gamma_{\mathcal{SF}}$, $\rho_{\mathcal{SF}}$	*Receiver SNR sensitivity and SIR sensitivity.*
Γ	*RSSI relay threshold.*
Φ, I_Φ	*Set of interferers, sum of instantaneous.*
$P_{SNR}(d)$	*SNR success probability at a distance d from GW.*
$P_{SIR}(d)$	*SIR success probability at a distance d from GW.*
$P_{\mathcal{SF}}(d)$	*Average success probability at distance d from GW.*
φ	*Average coverage probability.*

III. System Model

Assume a UL scenario in a LoRa network where a single GW is located at the center of a coverage area $\mathcal{C}$ with a radius of R_c, yielding an area denoted as $\mathcal{S} = \pi R_c^2$. Let $\{\mathbf{ED} = \mathcal{ED}_i | i \in \{1, \ldots, N\}\}$ defines the set of EDs, where N represents the total number of EDs. $\mathcal{C}$ is divided effectively into multiple disks on the basis of EAB SF-distance allocation scheme [30], as illustrated in Fig. 1(a). These disks comprise EDs distributed according to the Poisson point process with an intensity denoted by λ [31]. The notations used for the following derivations are listed in Table I.

TABLE II
LoRa Parameters at Bw = 125 kHz $CR = 4/8$

$\mathcal{SF}$	R (Kbps)	γ (dBm)	SNR (dB)	ρ (dB)
7	3.418	-123	-6	1
8	1.953	-126	-9	1
9	1.098	-129	-12	1
10	0.610	-132	-15	1
11	0.335	-134.5	-17.5	1
12	0.183	-137	-20	1

LoRa employs a physical-layer communication system that utilizes frequency-shifted chirps for establishing communication between the GW and EDs. In LoRa specification [6], a predefined set of pseudo-orthogonal SFs is defined as $\{\mathbf{SF} = \mathcal{SF}_k | k \in \{7, \ldots, 12\}\}$. Due to the spread spectrum nature of LoRa signals, each SF has a distinct minimum SNR (γ) required for successful decoding at the receiver, as shown in Table II. Generally, as the distance from the GW increases, the SNR of the transmitted signal decreases. Consequently, EDs located farther away from the GW are assigned higher SFs to ensure reliable connectivity. Within each disk of $\mathcal{C}$, the distributed EDs must use a specific SF to establish communication with the GW. The average surface between each SF region is denoted as $\lambda \mathcal{S}_{\mathcal{SF}} = \lambda\pi(d^2_{\mathcal{SF}} - d^2_{\mathcal{SF}-1})$. Another crucial parameter associated with SF is the transmission rate, measured in bits per second (bps), defined as

$$R_{\mathcal{SF}} = \frac{\mathcal{SF}}{2^{\mathcal{SF}}} \times \text{Bw} \times CR. \tag{1}$$

By assuming that each ED transmits the same packet length $L_{\mathcal{SF}}$, the packet duration for each SF is given by $T_{\mathcal{SF}} \triangleq L_{\mathcal{SF}}/R_{\mathcal{SF}}$. The packet duration determines the number of ED transmissions under the constraint of limited duty cycle (defined to be 0.1% or 1% by LoRaWAN specification [6]). Assume that the transmitted power P_i of the $\mathcal{ED}_i$ which is bounded by $P_{\max}$ and the transmitted signal between the GW and ED encounters a Raleigh fading channel, therefore the received signal strength at each end is given as [28]

$$R_x = P_i \times |h_{i,g}|^2 \times l(d) \tag{2}$$

where $|h_{i,g}|^2$ and $l(d)$ are the small-scale fading coefficient between $\mathcal{ED}_i$ and the GW, and the large-scale fading model, respectively. In this article, the Hata model presented in [32] is considered.

In the following sections, the relay model and its parameters are going to be defined along with the analysis of the proposed relay success probability. Finally, a problem definition is formulated with a proposed GA.

A. Relay Model

Assuming that it has a reliable communication link with the GW. The proposed relay model categorizes EDs based on their received signal parameters, namely, RSSI, $\mathcal{SF}$, and $\mathcal{FC}$ into three types. The first category consists of EDs that can reliably reach the GW directly without modifying their TxParams. The second category contains EDs that must modify their TxParams upon each wake-up to establish a direct communication link with the GW. Finally, the last one includes EDs located outside $\mathcal{C}$ and are unable to reach the GW even with maximum TxParams, as illustrated in Fig. 1(a). The relaying mechanism's details are further explained in Section IV.

B. Relay Parameters

Let $\{\mathbf{Z_r} | r \in \mathbf{SF}\}$ denote the region in $\mathcal{C}$ where the relay is going to be positioned. To perform optimally, the relay is geometrically efficiently placed at a position which satisfies the following constraints.

1) Ensures a reliable communication link with the GW.
2) Can receive the adjustable EDs signals before they reach the optimum TxParams.
3) Can reach the maximum number of unreachable EDs.

The relay TxPower $P_r \in [P_{r_{\min}}, P_{r_{\max}}]$ is bounded by ISM band maximum TxPower restriction [33]. P_r is adjusted such that the ED signal reaches with minimum decodable SNR level at the GW (Table II). Moreover, since there is no coordination between the relay and GW, the relay has no information when the other EDs are transmitting. Therefore, a limit on the relaying capacity (i.e., maximum relayed EDs within duration T) is required. In particular, to incorporate the proposed relay into a network, the optimum relay position $\mathbf{Z_r}$ that maximizes the success probability of the received signal at the GW should be determined while considering increasing the joint probability of SNR and SIR [34].

C. SNR and SIR Analysis

In order to derive the success probability in the proposed system model, the SNR and SIR analysis of single-hop LoRa transmission are performed.

1) SNR Analysis for Single-Hop LoRa: To model the SNR, we consider a system without interference between inter-SF or co-SF. For both UL or DL, a received signal is dropped or not received if it falls under the threshold $\gamma_{\mathcal{SF}} = N_0 + NF + 10\log_{10} B + SNR_{\mathcal{SF}}$, where $N_0 = -174$ dBm is the noise power density, NF is the noise figure, and $SNR_{\mathcal{SF}}$ is the minimum value where the signal is demodulated [30]. For a received signal power in (2), the SNR success probability of $\mathcal{ED}_i$ located at a distance $d_{i,g}$ from the GW is given by

$$\begin{aligned} P_{\text{SNR}}(d_{i,g}, \gamma_{\mathcal{SF}}) &= P\Big[P_i |h_{i,g}|^2 l(d_{i,g}) > \sigma^2 \gamma_{\mathcal{SF}}\Big] \\ &= \exp\left(-\frac{\sigma^2 \gamma_{\mathcal{SF}}}{P_i l(d_{i,g})}\right) \end{aligned} \tag{3}$$

where the channel gain $|h_{i,g}|^2$ is modeled as an exponential random variable with a unit mean, i.e., $|h_{i,g}|^2 \sim \exp(1)$ for all the channel links in the system and σ^2 is the variance of the additive white Gaussian noise (AWGN).

2) SIR Analysis for Single-Hop LoRa: Considering signal intensity and its interference in the absence of noise, the sum of instantaneous is defined as [31]

$$\mathbf{I}_{\Psi_i} = \sum_{q \in \Psi_i} P_q |h_{q,g}|^2 l(d_{q,g}) \tag{4}$$

where Ψ_i is the set of interferes and $d_{q,g}$ is the distance between the interfering ED and the GW. Therefore, the SIR of a signal transmitted from $\mathcal{ED}_i$ to the GW is defined as

$$\xi(\mathcal{ED}_i \longrightarrow GW|\Psi_i) = \frac{P_i|h_{i,g}|^2 l(d_{i,g})}{\mathbf{I}_{\Psi_i}}. \tag{5}$$

According to [35], the $\mathcal{ED}_i$ signal is successfully received if the SIR is greater than an established threshold ρ (Table II). Based on (5), the SIR success probability of $\mathcal{ED}_i$ located at a distance $d_{i,g}$ from the GW encountering an interference Ψ_i is given as

$$\begin{aligned} &P_{\text{SIR}}(d_{i,g}, \rho) \\ &= P\left[\frac{P_i|h_{i,g}|^2 l(d_{i,g})}{\mathbf{I}_{\Psi_i}} > \rho\right] = \exp\left(-\frac{\rho}{P_i l(d_{i,g})}\mathbf{I}_{\Psi_i}\right) \\ &= \exp\left(-2\pi\alpha_{\mathcal{SF}}\lambda \int_{d_{\mathcal{SF}-1}}^{d_{\mathcal{SF}}} \frac{\rho l(x)}{l(d_{i,g}) + \rho l(x)} x dx\right) \end{aligned} \tag{6}$$

where $\alpha_{\mathcal{SF}}\lambda$ is the transmission intensity of the PPP distributed in the LoRa network, and $\alpha_{\mathcal{SF}}$ is the regulated maximum duty cycle transmission.

D. Relay Analysis

Relay analysis is represented by two; the first involves the examination of SNR and SIR during the receiving phase of the relay, and the second pertains to the SNR and SIR of the signal phase forwarding.

1) Receiving Phase SNR and SIR: The relay position allows to receive signals from reachable EDs, unreachable EDs, and adjustable EDs. For unreachable devices which can communicate only with the relay, they are denoted differently $\{\mathbf{ED}' = \{\mathcal{ED}_m | m \in \{1, \ldots, M\}\}$, where $M \ll N$ since it is not realistic to have more EDs outside $\mathcal{C}$ area than within.

Let the relay SNR success probability of ED located at distance $d_{i,r}$ far from the relay denoted by P^r_{SNR}, which is calculated based on (11), as shown at the bottom of the page, and is given by

$$\begin{aligned} P^r_{\text{SNR}}(d_{i,r}, \gamma_{\mathcal{SF}}) &= P\left[P_{i/m}|h_{i/m,r}|^2 l(d_{i,r}) > \sigma^2 \gamma_{\mathcal{SF}}\right] \\ &= \exp\left(-\frac{\sigma^2 \gamma_{\mathcal{SF}}}{P_{i/m} l(d_{i,r})}\right). \end{aligned} \tag{7}$$

The notation i/m means that the received signal is from an ED within the area $\mathcal{C}$ or from outside the coverage area. Both $|h_{i/m,r}|^2$ and $l(d_{i,r})$ represent the small-scale fading and the large-scale attenuation between ED and the relay, respectively.

For the relay interference model, the SIR and ED encounter while transmitting to the relay is given by

$$\xi^r(\mathcal{ED}_{i/m} \longrightarrow \text{Relay}|\Psi') = \frac{P_i|h_{i/m,r}|^2 l(d_{i,r})}{\mathbf{I}_{\Psi'}} \tag{8}$$

where Ψ' represent the set of interfering signals from both $\mathcal{ED}_i$ and $\mathcal{ED}_m$, and $\mathbf{I}_{\Psi'}$ is the sum of instantaneous signal power, defined as

$$\mathbf{I}_{\Psi'} = \sum_{q \in \Psi_i} P_i|h_{q,r}|^2 l(d_{q,r}) + \sum_{q' \in \Psi_m} P_k|h_{q',r}|^2 l(d_{q',r}). \tag{9}$$

Based on (6), the SIR probability of success P^r_{SIR} of ED located $d_{x,r}$ far from the relay taking into account the set Ψ' is formulated as

$$\begin{aligned} &P^r_{\text{SIR}}(d_{i,r}, \rho) \\ &= P\left[\frac{P_i|h_{i/m,r}|^2 l(d_{i,r})}{\mathbf{I}_{\Psi'}} > \rho\right] = \exp\left(-\frac{\rho}{P_i l(d_{i/m,r})}\mathbf{I}_{\Psi'}\right) \\ &= \exp\left(-\frac{\rho}{P_i l(d_{i,r})}\mathbf{I}_{\Psi_i}\right) \times \exp\left(-\frac{\rho}{P_i l(d_{m,r})}\mathbf{I}_{\Psi_m}\right). \end{aligned} \tag{10}$$

Let the disk region of the unreachable ED bounded by an interval $[d_{\mathcal{SF}'-1}, d_{\mathcal{SF}'}]$, where $\{\mathbf{SF}' = \mathcal{SF}'_n | n \in \{7, \ldots, 12\}\}$. Using this notation, (10) can be expanded further to (11).

2) Transmission Phase SNR and SIR: For a signal forwarded from a relay that is located at a distance $d_{g,r}$ from the GW, the SNR success is given by

$$\begin{aligned} P^t_{\text{SNR}}(d_{g,r}, \gamma_{\mathcal{SF}}) &= P\left[P_r|h_{g,r}|^2 l(d_{g,r}) > \sigma^2 \gamma_{\mathcal{SF}} \mid a < \Gamma_{\mathcal{SF}}\right] \\ &= \exp\left(-\frac{\sigma^2 \gamma_{\mathcal{SF}}}{P_r l(d_{g,r})}\right) \exp\left(-\frac{\sigma^2 \Gamma_{\mathcal{SF}}}{P_{i/m} l(d_{i,r})}\right) \end{aligned} \tag{12}$$

where $a = P_{i/m}|h_{i/m,r}|^2 l(d_{i,r})$ indicates that the received signal by the relay is under the RSSI threshold and it requires forwarding. The SNR success probability of the relay DL to the EDs is beyond the scope of this work as it is assumed that the relay DL can reach to the EDs.

To reduce the potential of a collision occurring between the forwarded signal of the relay and the UL signals conveyed by other EDs, the relay employs a distinct channel frequency shuffling mechanism as explained in Section IV-C. Another aspects that should be taking into consideration is the mutual interference between the GW and the relay DL signals. Interference only affects EDs within area $\mathcal{C}$, as the GW DL signal to unreachable EDs is weak enough to interfere on the relay's DL signa. So, the SIR of a DL signal from relay encounters while it is broadcasted to the ED is given as

$$\xi^r(\text{Relay} \longrightarrow \mathcal{ED}_{i/m}|\Psi_g) = \frac{P_r|h_{i/m,r}|^2 l(d_{g,r})}{\mathbf{I}_{\Psi_g}} \tag{13}$$

where Ψ_g represents the set of interfering DL signals from the GW, and $\mathbf{I}_{\Psi_g}$ is the sum of instantaneous signal power which is defined as $\mathbf{I}_{\Psi_g} = P_g|h_{i,g}|^2 l(d_{i,g})$. Therefore, the SIR success

$$P^r_{\text{SIR}}(d_{i,r}, \rho) = \exp\left(-2\pi\alpha_{\mathcal{SF}}\lambda \int_{d_{\mathcal{SF}-1}}^{d_{\mathcal{SF}}} \frac{\rho l(x)}{l(d_{i,r}) + \rho l(x)} x dx\right) \exp\left(-2\pi\alpha_{\mathcal{SF}}\lambda \int_{d_{\mathcal{SF}'-1}}^{d_{\mathcal{SF}'}} \frac{\rho l(x)}{l(d_{i,r}) + \rho l(x)} x dx\right) \tag{11}$$

probability of relay DL signal while encountering DL from GW is given by

$$\begin{aligned} &P_{\mathrm{SIR}}\left(d_{i,r},\rho_{sf}\right)\\ &=P\left[\frac{P_r|h_{i,r}|^2 l\left(d_{g,r}\right)}{\mathbf{I}_{\Psi_g}}>\rho\right]=\exp\left(-\frac{\rho}{P_r l\left(d_{g,r}\right)}\mathbf{I}_{\Psi_g}\right)\\ &=\exp\left(-2\pi\alpha_g\frac{\left(d_{g,r}\right)}{l\left(d_{g,r}\right)+\left(d_{g,r}\right)}\right) \end{aligned} \tag{14}$$

where α_g is the regulated maximum duty cycle of the GW.

E. Relay Capacity Analysis

The relay's capacity, denoted as Ω, defines the maximum count of EDs the relay can manage within a time period T. In addition to relaying unreachable signals to the GW, the relay actively transmits DL signals to the EDs for acknowledgment. This assigns it the role of an active network device adhering to duty cycle restrictions. Functioning on the same channel as the GW for DL signals, limited to a 10% duty cycle, the relay's handling capacity within period T is restricted by the maximum number of DL packets it can transmit. According to [28], the maximum forwarded packets by the relay ED, satisfying the duty cycle are determined by

$$\begin{aligned} \Omega &\leq \frac{\alpha_g T}{ToA_{\mathcal{SF}}}\\ \Omega_{\max} &= \left\lceil \frac{\alpha_g T}{ToA_{\mathcal{SF}}} \right\rceil. \end{aligned} \tag{15}$$

F. Problem Formulation

Within this section, we present the formulation of an optimization problem aimed at maximizing the coverage probability and success probability of both the GW and the relay, by finding the optimum relay region as a Pareto solution.

In order to determine the coverage probability of either the GW or the relay, we begin by establishing the average success probability of an ED communicating with either the relay or the GW. To accurately model the success probability of the proposed system, the combined influence of SNR and SIR requirements is evaluated. Following the methodology outlined in [31], the success probability is derived based on calculating the joint probability of achieving both the specified SNR and SIR conditions, as expressed in

$$P^{\mathrm{suc}}_{\mathcal{SF}}(x)=P_{\mathrm{SNR}}(x)\times P_{\mathrm{SIR}}(x). \tag{16}$$

Based on (16), the success probability of both relay $P^r_{\mathcal{SF}}$ and GW $P^g_{\mathcal{SF}}$ is given below by (17) and (18) as shown at the bottom of the page, respectively.

Formulas (17) and (18) are going to be denoted as $P^r_{\mathcal{SF}}(Z_r)$ and $P^g_{\mathcal{SF}}(Z_r)$, respectively, for the sake of simplicity and to highlight that $\{Z_r\}$ is the optimization variable.

Let $A(x)=1/(d_{\mathcal{SF}}-d_{\mathcal{SF}-1})$ be the probability density function (PDF) of the likelihood of finding an ED in its corresponding SF region and $B(x)=2\pi x/S$ be the likelihood of finding a certain number of EDs in area S. Using $A(x)$ and $B(x)$, we define the average success probability and the average coverage probability as in [28]. First, the average success probability for the relay is expressed as

$$\begin{aligned} \overline{P^r_{\mathcal{SF}}}|_{Z_{\mathcal{SF}}} &= \int_{Z_{\mathcal{SF}}} P^r_{\mathcal{SF}}(Z_r)A(x)dx\\ &= \int_{d_{\mathcal{SF}-1}}^{d_{\mathcal{SF}}} P^r_{\mathcal{SF}}(Z_r)\frac{1}{d_{\mathcal{SF}}-d_{\mathcal{SF}-1}}dx \end{aligned} \tag{19}$$

next the average success probability for the GW is given as

$$\begin{aligned} \overline{P^g_{\mathcal{SF}}}|_{Z_j} &= \int_{Z_i} P^g_{\mathcal{SF}}(Z_r)A(x)dx\\ &= \int_{d_{\mathcal{SF}-1}}^{d_{\mathcal{SF}}} P^g_{\mathcal{SF}}(Z_r)\frac{1}{d_{\mathcal{SF}}-d_{\mathcal{SF}-1}}dx. \end{aligned} \tag{20}$$

The respective average coverage probability expressions for relay and GW are given in (21), as shown the bottom of the page, and (22), as shown the bottom of the next page, respectively.

Based on the analysis models done in (19)–(22), a relaying mechanism is proposed which increases 1) the average success probability given in (17) and (20) and 2) along with the average coverage probability given by (21) and (22). Thus, the proposed system model's maximization problem is structured as

$$\begin{aligned} \underset{Z_r}{\operatorname{argmax}}\ \ &\mathcal{E}_r(Z_r)=\zeta_1\overline{\varphi^r_{Z_k}}\\ &+(1-\zeta_1)\min\left(\left\{\overline{P^r_{\mathcal{SF}}}|_{Z_k}\mid \quad \forall Z_k\in\mathbf{SF}\right\}\right) \end{aligned} \tag{23}$$

$$\begin{aligned} \underset{Z_r}{\operatorname{argmax}}\ \ &\mathcal{E}_g(Z_r)=\zeta_2\overline{\varphi^g_{Z_k}}\\ &+(1-\zeta_2)\min\left(\left\{\overline{P^g_{\mathcal{SF}}}|_{Z_k}\mid \quad \forall Z_k\in\mathbf{SF}\right\}\right) \end{aligned} \tag{24}$$

$$P^r_{\mathcal{SF}}\left(d_{i,r}\right)=\exp\left(-\frac{\sigma^2\gamma_{\mathcal{SF}}}{P_{i/m}l\left(d_{i,r}\right)}\right)\exp\left(-2\pi\alpha_{\mathcal{SF}}\lambda\int_{d_{\mathcal{SF}-1}}^{d_{\mathcal{SF}}}\frac{\rho l(x)}{l\left(d_{i,r}\right)+\rho l(x)}xdx\right)\exp\left(-2\pi\alpha_{\mathcal{SF}}\lambda\int_{d_{\mathcal{SF}'-1}}^{d_{\mathcal{SF}'}}\frac{\rho l(x)}{l\left(d_{i,r}\right)+\rho l(x)}xdx\right) \tag{17}$$

$$P^g_{\mathcal{SF}}(d_{i,j})=\exp\left(-\left[\frac{\sigma^2\gamma_{\mathcal{SF}}}{P_i l\left(d_{i,g}\right)}+\frac{\sigma^2\gamma_{\mathcal{SF}}}{P_r l\left(d_{g,r}\right)}+\frac{\sigma^2\Gamma}{P_{i/m}l\left(d_{i,r}\right)}\right]\right)\exp\left(-2\pi\alpha_g\frac{\rho l\left(d_{i,g}\right)}{l\left(d_{i,r}\right)+\rho l\left(d_{i,g}\right)}\right)\exp\left(-2\pi\alpha_{\mathcal{SF}}\lambda\int_{d_{\mathcal{SF}-1}}^{d_{\mathcal{SF}}}\frac{\rho l(x)}{l\left(d_{i,g}\right)+\rho l(x)}xdx\right) \tag{18}$$

$$\overline{\varphi^r_{Z_k}}=\mathbb{E}|_{\forall Z_k}\left[P^r_{\mathcal{SF}}(Z_r)\right]=\sum_{\forall Z_k\in\mathbf{SF}}\left[\int_{d_{\mathcal{SF}}}^{d_{\mathcal{SF}-1}}P^r_{\mathcal{SF}}(Z_r)B(x)dx\right]=\sum_{\forall Z_k\in\mathbf{SF}}\left[\int_{d_{\mathcal{SF}}}^{d_{\mathcal{SF}-1}}P^r_{\mathcal{SF}}(Z_r)\frac{2\pi x}{S_{\mathcal{SF}}}dx\right] \tag{21}$$

$$\text{s. t.} \quad C1: Z_7 < Z_r < Z_{12}$$
$$C2: \Omega < \Omega_{\max}$$
$$C3: P_r \leq P_{\max} \quad \text{ISM band constraint} \tag{25}$$

where $\mathcal{E}_r$ and $\mathcal{E}_g$ are the relay and GW objective functions, respectively. The used weight factors in this optimization problem are indicated by ζ_1 and ζ_2 where they indicate the tradeoff between the success probability of each SF region and coverage probability.

Based on [36] and the objectives defined in (21) and (24), a multiobjective optimization problem is formulated with a set of constraints. The first constraint C1 indicates that the relay must be located within regions from Z_7 to Z_{12} region; the second constraint is the limited number of relayed devices Ω; and the last constraint C3 is related to the maximum power of ISM band relay devices restriction.

According to [37], the structured problem is a discrete nonconvex multiobjective problem, in which we are going to apply a GA to find the optimal Pareto solution, which is represented in the next section.

G. Proposed Genetic Algorithm

Multiobjective optimization problems present unique challenges due to their complex nature and inherent tradeoffs between objectives. Unlike single-objective approaches that seek a single optimal solution, multiobjective methods aim to identify a set of Pareto-optimal solutions that optimize all objectives simultaneously. Various techniques have emerged to tackle this challenge, including evolutionary algorithms like nondominated sorting genetic algorithm (NSGA)-II, which effectively explores diverse optimal solutions through genetic operators and dominance-based ranking [37].

In order to implement the NSGA-II in the suggested system model, it is important to clearly specify both the variables and objectives of the optimization problem. Let $\mathcal{P}$ be the collection of variables, defined as $\mathcal{P} \triangleq \{Z_r\}$. Additionally, let *PoP* represent the population size that will be tested under various selection ratios in order to determine the optimal performance while minimizing complexity. As depicted in Algorithm 1, the NSGA-II's overall methods encompass multiple steps, with the following steps being of utmost significance.

1) Objective Functions: Building on (23) and (24), the fitness functions of the NSGA-II that optimize both the success probability of each ED and the coverage probability of both the relay and GW. These combined goals drive the NSGA-II algorithm are expressed as

$$\mathcal{F}_{x_1} = \zeta_1 \overline{\varphi^r_{Z_k}} + (1-\zeta_1)\min\left(\left\{\overline{P^r_{\mathcal{SF}}}|_{Z_k} \mid \quad \forall Z_k \in \mathbf{SF}\right\}\right) \tag{26}$$

Algorithm 1: Optimize Relay Parameters Using NSGA-II

Output: $\mathcal{F}_{i,g}, \mathcal{P}_{opt}$
Initialization: Counter $t = 0$; Maximum generation$= M$, Random Population
$\mathcal{P} \leftarrow P_i | \forall i \in \{1, \ldots, PoP\}$

```
Define the fitness functions:
    F_{x1} ← {E_r(P_i) | P_i ∈ P}
    F_{x2} ← {E_g(P_i) | P_i ∈ P}
Procedure steps:
    while t ≤ M do
        P̂ ← Selection (P_i, F_{i,g}, PoP)
        P ← P̂
        for k = 1 ... PoP do
            P^k ← Crossover(P_{p1}; P_{p2})
            P^k ← Mutation (P^k)
            P^k ← Evaluation (P^k)
            P̃ ← Merge (P; P^k)
        P(t+1) ← Survivor (P̃; P)
        t = t + 1
(F_{i,g}, P_opt) ← (max F_{i,g}, argmax_P F_{i,g}):
```

$$\mathcal{F}_{x_2} = \zeta_2 \overline{\varphi^g_{Z_k}} + (1-\zeta_2)\min\left(\left\{\overline{P^g_{\mathcal{SF}}}|_{Z_k} \mid \quad \forall Z_k \in \mathbf{SF}\right\}\right). \tag{27}$$

2) Crossover: Following the randomized selection of the population size, the binary tournament selection algorithm is utilized to extract parent individuals from the current population, *PoP*, and generate a new generation for breeding [37]. Subsequently, a crossover operation is performed on this new population to foster diversification and potentially enhance the solution space exploration.

3) Survivor: After applying the mutation to the offspring solutions, evaluate their values using the fitness functions. Next, a survivor mechanism is applied to choose between the offspring solutions and the parent solutions based on Pareto dominance ranking.

IV. Relaying Mechanism

Upon determining the placement of the relay, an essential task is performed comprising the computation of RSSI, $\mathcal{SF}$, and the $\mathcal{FC}$ of the EDs received signals. In the case of class A LoRa sensors (which are considered in this article), two reception windows are activated for a limited duration subsequent to each UL transmission. Hence, it becomes crucial to capture one of these windows effectively. To accomplish this, it is necessary to ascertain the aforementioned parameters without the need for decoding the transmitted frame, prioritizing efficiency and speed, particularly in relation to $\mathcal{SF}$. In our

$$\overline{\varphi^g_{Z_k}} = \mathbb{E}|_{\forall Z_i}\left[P^g_{\mathcal{SF}}(Z_r)\right] = \sum_{\forall Z_k \in \mathbf{SF}}\left[\int_{d_{\mathcal{SF}}}^{d_{\mathcal{SF}-1}} P^g_{\mathcal{SF}}(Z_r)B(x)dx\right] = \sum_{\forall Z_k \in \mathbf{SF}}\left[\int_{d_{\mathcal{SF}}}^{d_{\mathcal{SF}-1}} P^g_{\mathcal{SF}}(Z_r)\frac{2\pi x}{S_{\mathcal{SF}}}dx\right] \tag{22}$$

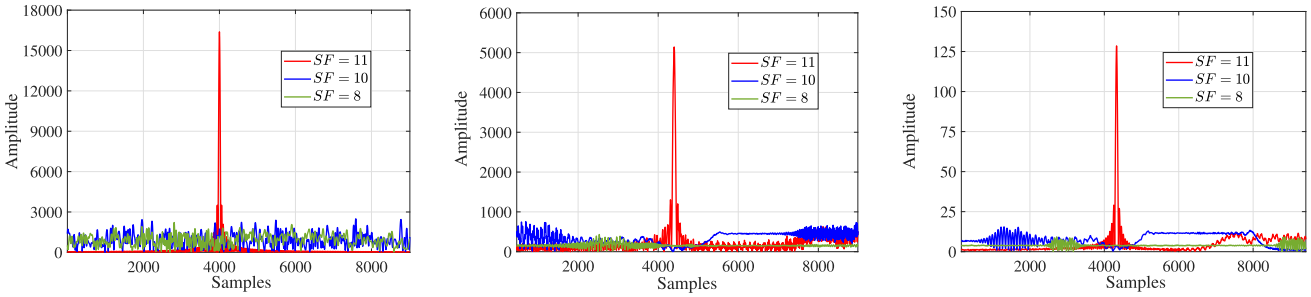

Fig. 2. Correlation results between the received signal and bank of preambles. (a) Simulated signal. (b) SX1276 generated signal with SNR = −24 dBm. (c) SX1276 generated signal with SNR = −63 dBm.

approach, we employ a correlation-based technique to infer the $\mathcal{SF}$. This technique involves correlating the received signal with a collection of parallel preambles associated with the six potential $\mathcal{SF}$ values. In the following subsections, parameters extraction and the proposed adaptive relaying mechanism which is summarized in Fig. 3 are explained thoroughly.

A. Parameters Extraction

The preamble is composed of eight up unmodulated chirps which can be represented as

$$P^{\mathcal{SF}_{\tilde{j}}}(t) = \sum_{m=1}^{8} \frac{1}{\sqrt{T_s^{\mathcal{SF}_{\tilde{j}}}}} e^{j2\pi\left(f_c + \frac{\mathcal{B}t}{2^{(\mathcal{SF}_{\tilde{j}}+1)}T}\right)t} \operatorname{rect}\left(\frac{t - mT_s^{\mathcal{SF}_{\tilde{j}}}}{T_s^{\mathcal{SF}_{\tilde{j}}}}\right) \tag{28}$$

where f_c is the starting frequency, the symbol duration is $T_s^{\mathcal{SF}_{\tilde{j}}} = 2^{\mathcal{SF}_{\tilde{j}}}T$ and $T = [1/(\mathrm{Bw})]$ with $\mathrm{Bw} \in \{125, 250\}$ kHz. From [38], the received LoRa signal can be written as

$$S_r^{\mathcal{SF}_{\tilde{i}}}(t) = \sum_{n=1}^{N_{\mathcal{P}}} \frac{1}{\sqrt{T_s^{\mathcal{SF}_{\tilde{i}}}}} e^{j2\pi\phi_n^{\tilde{k}}(t)} \operatorname{rect}\left(\frac{t - nT_s^{\mathcal{SF}_{\tilde{i}}}}{T_s^{\mathcal{SF}_{\tilde{i}}}}\right) \tag{29}$$

where $N_{\mathcal{P}}$ is the number of symbols in the received signal, $\phi^{\tilde{i}}(t)$ represents the instantaneous phase of symbol $\tilde{i}$ given by

$$\phi^{\tilde{k}}(t) = \begin{cases} \frac{1}{\sqrt{T_s}} e^{j2\pi\left(f_c + \frac{B}{2^{\mathcal{SF}_{\tilde{j}}}}\left(\frac{t-t_0}{2T} + \tilde{k}\right)\right)(t-t_0)}, & \text{for } 0 \le t - t_0 \le t_{\tilde{k}} \\ \frac{1}{\sqrt{T_s}} e^{j2\pi\left(f_1 + \frac{B}{2^{\mathcal{SF}_{\tilde{j}}}}\left(\frac{t-t_0}{2T} + \tilde{k} - 2^{\mathcal{SF}_{\tilde{j}}}\right)\right)(t-t_0)}, & \text{for } t_{\tilde{k}} \le t - t_0 \le T_s. \end{cases} \tag{30}$$

The cross-correlation of the received signal with the preamble of $\mathcal{SF}_{\tilde{j}}$ is written as

$$\mathcal{R}^{\mathcal{SF}_{\tilde{j},\tilde{i}}}(\tau) = \int_{\tau}^{N_{\mathcal{P}}T_s^{\mathcal{SF}_{\tilde{i}}}} S_r^{\mathcal{SF}_{\tilde{i}}}(t) P^{\mathcal{SF}_{\tilde{j}}}(t-\tau)^* dt \tag{31}$$

thus, the transmitted $\mathcal{SF}_{\tilde{i}}$ is the maximized correlation output represented as follows:

$$\mathcal{SF}_{\tilde{i}} = \arg\max_{\{\tilde{j}\}} \left\| \mathcal{R}^{\mathcal{SF}_{\tilde{j},\tilde{i}}} \right\|. \tag{32}$$

Note that since the preamble length for $\mathcal{SF} = 12$ is larger than the transmitted signal length for $\mathcal{SF} = 7$, the whole transmitted frame must be associated with the preamble.

Fig. 2(b) depicts the results of a received signal ($\mathcal{SF} = 11$) that is associated with a bank of preambles provided by (28). The correlation-based technique continually shows consistency in properly estimating the sent $\mathcal{SF}$, as evidenced by simulation results [Fig. 2(a)] and when examining received real transmitted signals [Fig. 2(b) and (c)]. Notably, even at low SNR values (−63 dBm), the relay accurately detects the SF of the signal.

The assessment of $\mathcal{FC}$ requires employment of suitable frequency filters. Likewise, the RSSI is accurately determined by utilizing a cost-effective implementation of filtered samples RSSI reporting integrated into SX1276 SEMTECH chips.

B. Link Budget

After computing the RSSI, $\mathcal{FC}$, and the $\mathcal{SF}_{\tilde{i}}$, the relay node categorizes the EDs into three groups: 1) reachable; 2) nonreachable; and 3) adjustable. The relay is strategically positioned to establish a dependable connection with the GW utilizing various SFs. Then, the path loss (PL) denoted as $l(d)$, between the GW and the relay is accurately determined while accounting for an uncertainty margin of $\delta^{\mathcal{SF}_{\tilde{i}}}$ associated with $\mathcal{SF}_{\tilde{i}}$. The relay node performs link budget calculations to assess the feasibility of communication between the GW and the EDs, such as

$$L_{\mathcal{SF}_{\tilde{i}}} = \mathrm{RSSI}_{\mathcal{SF}_{\tilde{i}}} + l\left(d_{g,r}\right) + \delta_{\mathcal{SF}_{\tilde{i}}}. \tag{33}$$

For a given $L_{\mathcal{SF}_{\tilde{i}}}$, the relay classifies the EDs as

$$\begin{cases} \left|S_{\mathcal{SF}_{\tilde{i}}}^{\mathrm{Bw}_k}\right| \ge \left|L_{\mathcal{SF}_{\tilde{i}}}\right|, & \text{Reachable ED} \\ \left|S_{\mathcal{SF}_{12}}^{\mathrm{Bw}_k}\right| < \left|L_{\mathcal{SF}_{\tilde{i}}}\right|, & \text{Unreachable ED} \\ \left|S_{\mathcal{SF}_{12}^{\mathrm{Bw}_k}}\right| \le \left|L_{\mathcal{SF}_{\tilde{i}}}\right| < \left|S_{\mathcal{SF}_{\tilde{i}}^{\mathrm{Bw}_k}}\right|, & \text{Adjustable ED} \end{cases} \tag{34}$$

where $S_{\mathcal{SF}_{\tilde{i}}}^{\mathrm{Bw}_k}$ corresponds to the sensitivity of $\mathcal{SF}_{\tilde{i}}$ transmitted at Bw_k, in the rest of this article, Bw_k is chosen to be 125 kHz. The operational behavior of the relay with respect to reachable and unreachable EDs is illustrated in Fig. 3. In scenarios where sensors are within the communication range of the GW, the relay remains passive and does not participate in the data transmission. Conversely, for EDs located beyond the GW's reach, the relay behaves as a conventional repeater device,

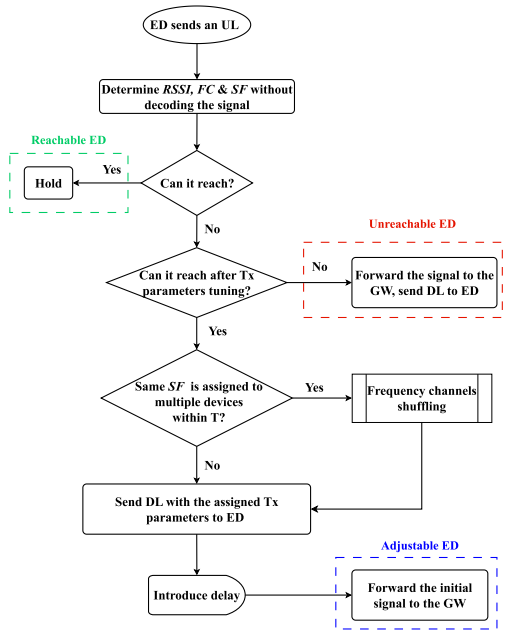

Fig. 3. Flowchart of the proposed relaying mechanism.

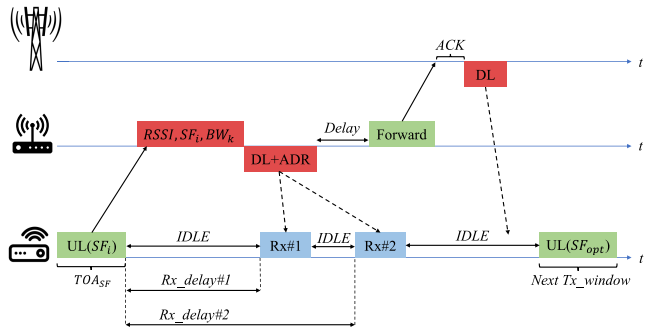

Fig. 4. Timeline of adjustable class A EDs TxParams tuning through relaying node.

continuously forwarding the data packets between the ED and the GW. In the last scenario, the relay confines the sensor to the lowest possible $\mathcal{SF}$ which allows it to detect the signal from the out-of-reach ED.

In the case of configurable nodes, the relay selects the best $\mathcal{SF}$ for the next transmission window, denoted as $\mathcal{SF}^{\text{opt}}$. After that, the ADR bit is enabled in the DL frame to allow the TxParams adjustment MAC instructions to be sent, as illustrated in Fig. 4. The relay uses a lookup table to find the suitable $\mathcal{SF}^{\text{opt}}$ and calculates the link budget using (33). $\mathcal{SF}^{\text{opt}}$ is chosen as the minimal $\mathcal{SF}$ that assures the signal reaches the GW while meeting the link budget requirements, such as

$$\mathcal{SF}^{\text{opt}} = \min\left\{\mathcal{SF}_{\tilde{i}} | \quad |S^{\text{Bw}}_{\mathcal{SF}_{\tilde{i}}}| \geq |L_{\mathcal{SF}_{\tilde{i}}}|\right\}. \tag{35}$$

C. FC Assignment

EDs typically store data and transmit it in multiple packets sequentially within a time interval T. Then, once the relay receives the first UL frame from a particular node, it assumes that the same node will transmit subsequent data packets within

Algorithm 2: FCs Shuffling Algorithm

Input : $\{\mathbf{FC} = \mathcal{FC}_j | j \neq \bar{j} \in \{1, \ldots, 8\}\}$,
$\{\mathbf{ED} = \mathcal{ED}_i | i \in \{1, \ldots, N\}\}$,
$\{\mathbf{SF} = \mathcal{SF}^{\text{opt}}_k | k \in \{7, \ldots, 12\}\}$,
Initialization: Counter $t = 0$; T; $j = 1$.

```
Arrays assignment:
    SF ← (ED_1, SF^opt_{k,1})
    FC ← (ED_1, FC_1)
Frequency assignment:
    while t ≤ T do
        for i = 2:N do
            if SF(ED_{i-1}, SF^opt_{k,i-1}) = SF(ED_i, SF^opt_{k,i}) then
                FC ← (ED_i, FC_{[j+1]_|FC|})
            else
                FC ← (ED_i, FC_j)
            end
        end
    end
    t → t = 0;
```

the following T seconds. Thus, when a group of EDs are assigned with the same $\mathcal{SF}^{\text{opt}}$ within T, the relay shuffles their $\mathcal{FC}$s in the coming transmissions to prevent collisions, this procedure is described in Algorithm 2.

As the signal forwarding by the relay is more frequent, a nondefault transmission channel, $\mathcal{FC}_{\tilde{j}}$, is reserved exclusively for the relay's transmissions. This ensures that the signals from the relay will not interfere with the normal operation of other EDs either at the initial or post-adaptation phase.

V. Performance Analysis

In this section, the proposed positioning algorithm and the relaying mechanism are analyzed in terms of convergence, throughput, power, and ToA savings.

A. Algorithm Convergence

The evaluation of the NSGA-II algorithm's efficacy involves monitoring its convergence toward Pareto-optimal solutions. This convergence is assessed by tracking changes in the fitness function as the number of generations progresses [39]. Fig. 5 illustrates the convergence of the fitness function across varying mutation rates, μ, and intensity of EDs, λ, while maintaining ζ at a value of 0.5 for algorithmic simplicity. A lower μ corresponds to a gradual convergence rate due to constrained exploration of the search space. This cautious approach may result in the algorithm being trapped in local optima. Conversely, employing a higher μ facilitates faster convergence but may impede thorough investigation of the most favorable regions due to rapid random movements. Hence, selecting an optimal μ necessitates balancing the convergence rate and the extent of exploration in the search space. Additionally, from Fig. 5, it is observed that an increase in λ drives the fitness function toward reduced values owing to heightened network interference. Optimal selection of the pair

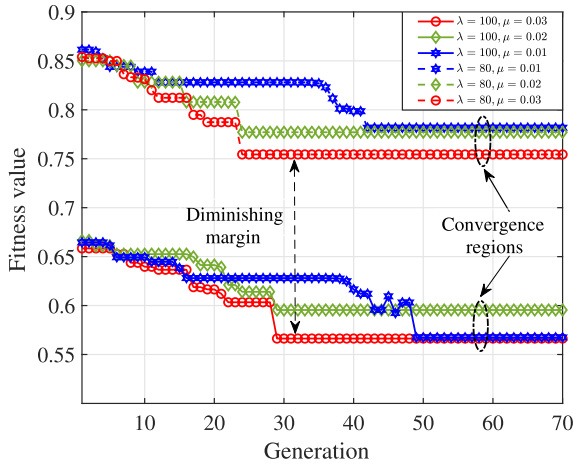

Fig. 5. NSGA-II fitness function convergence.

μ, λ ensures that the fitness function of the proposed algorithm consistently converges to two Pareto solutions, specifically in the regions where $\mathcal{SF} = 9, 10$. Consequently, the subsequent discussion in this article confines the relay's position to these two regions.

B. Throughput

The throughput of a single ED is modeled as a function of the probability of success $\overline{P^r_{\mathcal{SF}}}$ and the duty cycle $\alpha_{\mathcal{SF}}$ along with the data rate of each SF $R_{\mathcal{SF}}$ [34], so the throughput of single ED is given by

$$\Theta_{\mathcal{SF},i} \triangleq R_{\mathcal{SF}} \times \alpha_{\mathcal{SF}} \times P^{\text{suc}}_{\mathcal{SF}}. \tag{36}$$

Based on (36), the total network throughput is defined as the average sum of all EDs that can establish a communication with the GW and is given as

$$\Theta_T \triangleq \frac{1}{S'}\mathbb{E}\left(\sum_{\mathcal{ED}_i \in S'} \Theta_{\mathcal{SF},i}\right) \tag{37}$$

where S' is the union set of the reachable, adjustable, and unreachable EDs in the network.

C. Adaptive Relaying

Let $\mathcal{SF}^{\text{init}}_i$ denote the SF at which the relay can detect the signal from $\mathcal{ED}_i$, and $\mathcal{SF}^{\text{opt}}_i$ represent the minimum SF determined by the relay for the ith ED to communicate directly with the GW. The degree difference between the initial and optimum SFs is given by

$$\mathcal{L}^{\text{init}}_i = \mathcal{SF}^{\text{opt}}_i - \mathcal{SF}^{\text{init}}_i \tag{38}$$

utilizing the adaptive relaying mechanism, the relay conserves $\sum_{\bar{i}=0}^{\mathcal{L}^{\text{init}}_i - 1} T^{\mathcal{SF}^{\text{init}}_i + \bar{i}}$ of the ToA for the ith node. Similarly, let $\mathcal{P}^{\text{unit}}_{\mathcal{SF}_k}$ denote the power consumed per symbol using $\mathcal{SF}_k$. The power saving for device i can be expressed as

$$\mathcal{P}^{\text{savings}}_i = \sum_{\bar{i}=0}^{\mathcal{L}^{\text{init}}_i - 1} \bar{N}\mathcal{P}^{\text{unit}}_{\mathcal{SF}_{k+\bar{i}}} \tag{39}$$

where $\bar{N}$ represents the number of symbols transmitted in a frame using $\mathcal{SF}_k$.

D. Amplification Ratio

Rather than indiscriminately amplifying the forwarded signal, the relay dynamically adjusts the amplification power ratio $\mathbb{A}$ in accordance with a predetermined value derived from (33). This ensures that every transmitted signal achieves an optimal RSSI at the GW, allowing it to be successfully decoded. The optimal RSSI, denoted by RSSI^{opt}, is defined as

$$\left|\text{RSSI}^{\text{opt}}\right| \leq \left|S^{\text{Bw}}_{\mathcal{SF}_k}\right| - \left|l(d_{i,r}) + \delta_{\mathcal{SF}_k}\right|. \tag{40}$$

Since (40) is presented in logarithm form, its linear form is presented as

$$\text{linear}\left(\left|\text{RSSI}^{\text{opt}}\right|\right) \leq \frac{\text{linear}\left(\left|S^{\text{Bw}}_{\mathcal{SF}_k}\right|\right)}{\text{linear}\left(\left|l(d_{i,r})||\delta_{\mathcal{SF}_k}\right|\right)}. \tag{41}$$

The amplification ratio $\mathbb{A}$ is defined as the ratio between RSSI^{opt} and the calculated RSSI

$$\mathbb{A} = \frac{\text{linear}\left(\left|\text{RSSI}^{\text{opt}}\right|\right)}{|\text{RSSI}|} + \kappa. \tag{42}$$

Due to variation of attenuation levels and hardware impairments (low-end devices), an offset value of κ is added to ensure the signal is amplified to a level where it can be decoded by the GW, while achieving the highest possible power efficiency.

VI. Simulation Results

This section validates the accuracy of analytical models through MATLAB simulation within a 30-km radius cell with an intensity of 300 EDs per square kilometer. The simulations consider European Union regional parameters, including $f_c =$ 868 MHz, $Bw = 125$ kHz, and Txpowers of $P_i = 14$ and $P_r = 25$ for the EDs and relay, respectively. The packet length is set to 115 Bytes to accommodate various data rates (DR0, DR1, DR2, and DR3) along with CR, duty cycle, and noise figure of 4/8, 0.1%, and -117 dBm, respectively. Throughout the simulation, the EDs are distributed using PPP distribution and EAB-$\mathcal{SF}$s-based allocation.

A. Impact on Success and Outage probability

Fig. 6 illustrates $P^{\text{suc}}_{\mathcal{SF}}$ as a function of the ED distance; the periodic abrupt change in the decreasing behavior of $P^{\text{suc}}_{\mathcal{SF}}$ is due to the change of γ from $\mathcal{SF}$ to another (Table II). Additionally, the relay positioning at the region $\mathcal{SF} = 9$ results in the convergence of $P^{\text{suc}}_{\mathcal{SF}}$ to a better value compared to the single-hop network [31] in which the network $P^{\text{suc}}_{\mathcal{SF}}$ tends to decay rapidly affected by the transmitted packet SNR and SIR levels degradation due to the PL increase for larger cell radius associated with the interference generated by longer packet length as higher $\mathcal{SF}$ are adopted. In contrast, the proposed scheme exploits the joint maximization SNR and SIR using the amplification feature (42) and the FCs shuffling algorithm,

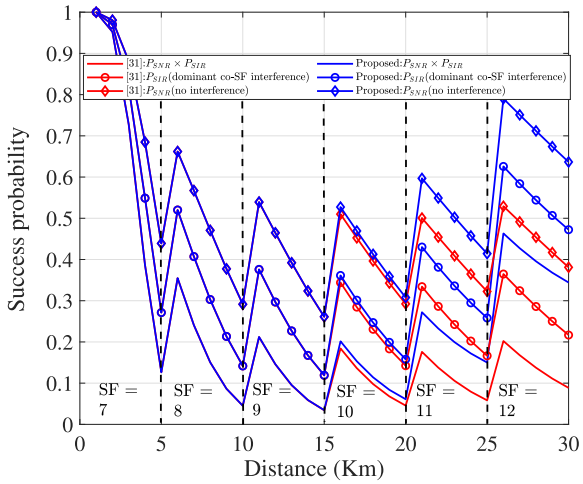

Fig. 6. Success probability under different SIR conditions per SF region, for $N = 200$.

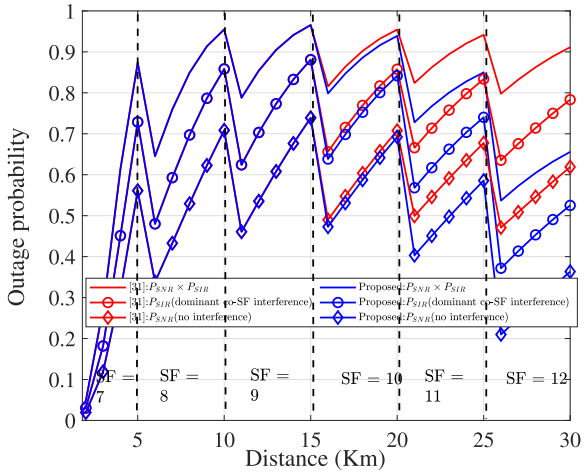

Fig. 7. Outage probability performance inside GW coverage area per SF region, for $N = 200$.

respectively. Furthermore, the network reliability is assessed in terms of the outage probability as

$$P^{\text{outage}} = 1 - P^{\text{suc}}. \tag{43}$$

The proposed relaying mechanism exploits its ability to adjust the TxParams of EDs, where Fig. 7 depicts that a gain of 40% in P^{outage} is achieved compared to the single-hop network [31].

Since the relay can only forward the signals of the unreachable devices without altering their TxParams, the P^{suc} of these EDs is expected to behave as the P^{suc} of a single-hop network, which is confirmed in Fig. 8 that illustrates also the network coverage area is extended up to 50%, approximately.

B. Impact on ToA and Data Rate

Fig. 9 shows that as the relay adjust the TxParams of the adjustable EDs during the initialization process, it avoids wasting ToA and optimizes the data rate. For instance, when the relay assigns an optimal SF of 11 to a received signal with an SF of 9, it results in a fourfold increase in saved ToA

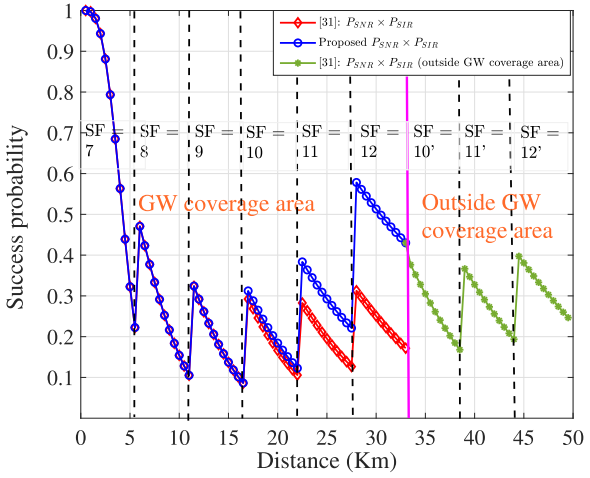

Fig. 8. Success probability under different SIR conditions per SF region for unreachable devices.

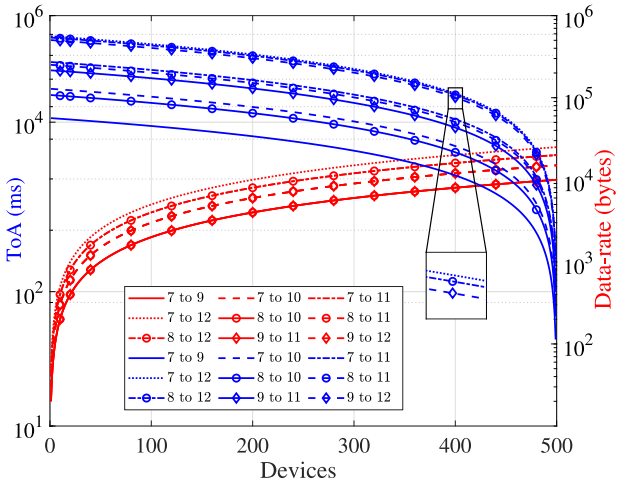

Fig. 9. ToA and data rate saving based on different SF adaptation scenarios.

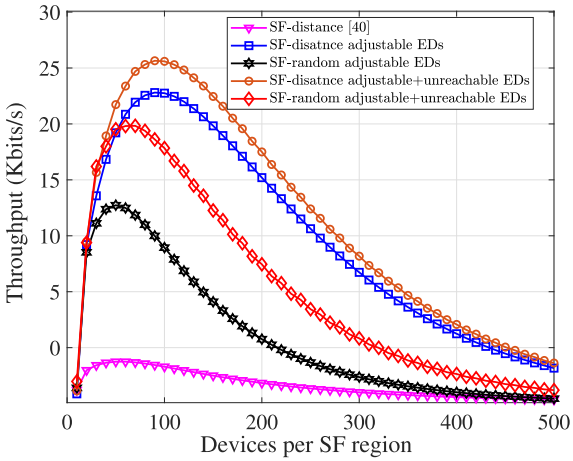

Fig. 10. Average network throughput for different SF allocation schemes.

for a single ED. When applied to a larger number of EDs, this method drastically reduces the total amount of wasted ToA.

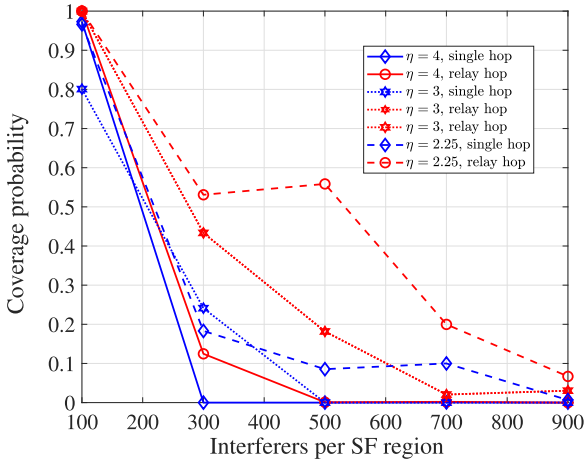

Fig. 11. Total coverage probability with respect to average number of interferers per SF region.

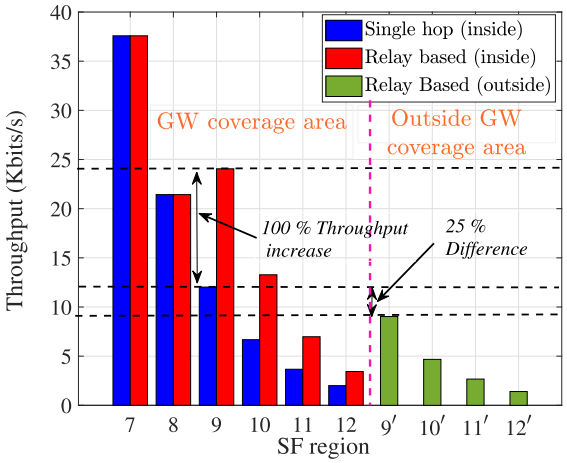

Fig. 13. Average throughput per SF region with and without the relaying scheme, for $N = 200$.

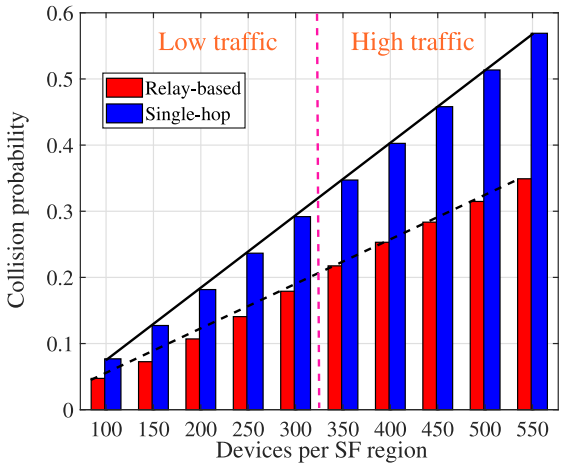

Fig. 12. Network collision probability with and without the FCs shuffling algorithm.

C. Impact on Throughput

The assessment of the network throughput is directly related to P^{suc} as indicated in (36). So, by projecting the ability of the proposed relaying scheme to enhance the $P^{\text{suc}}_{\mathcal{SF}}$, Fig. 13 illustrates that starting from $\mathcal{SF} = 9$ where the relay is positioned the throughput among the adjustable devices is doubled compared to single-hop network, making the throughput distribution more uniform across the network in contrast to standard LoRa networks that suffer from nonuniform throughput distribution among $\mathcal{SF}$ regions.

Based on (37), the increase of EDs number in the network directly affects the total throughput in the network due the degradation of the SIR level. In Fig. 10, the throughput performance under the different SF allocation schemes (EAB scheme and EIB scheme) of the proposed scheme is depicted where it reaches a maxima approximately 25 kb/s, unlike the single-hop network in [40] that is saturated at a total throughput maximum of 5 kb/s. This margin gain of 20 kb/s is attributed to the ability of the proposed scheme to keep a reliable level of SIR through the FC shuffling mechanism and the feature of scheduling along with power amplifying. In addition, the slower decrease rate of throughput compared to [40] is projected on to the uniform and gradual rise in collision probability, as demonstrated in Fig. 12.

D. Impact on Coverage Probability

The suggested relay mechanism forms its decision-making process by integrating a PL model denoted as $l(d)$. This model necessitates fine-tuning, a process contingent upon the specifics of the deployed network environment. Referring to Fig. 11, the impact of varying η values becomes apparent in relation to the coverage probability outlined in (21) and (22). As anticipated, rural locales characterized by lower η values exhibit superior coverage while encompassing a greater number of EDs when compared to urban areas characterized by higher η values.

E. Experimental Results

Within this part, an assessment is conducted on the execution of the relay scheme that has been put forward. The GW and LoRa nodes employ an ESP32 LiLyGo T-beam integrated with an SX1276 LoRa module, and the relay algorithm is implemented on a USRP E310 device. For the experiment setup, the equipment are distributed on the top of Istanbul Medipol university campus as shown in Fig. 14(a). Three nodes A, B, and C (red dots) are used as EDs distributed with different distances and different heights from the GW (orange dot). While the relay (black dot) is positioned in a line of sight with GW and in a reliable position with the other nodes.

To investigate the impact of initial LoRa network communication stage. First, a conventional network without relay is established, where each node transmits one thousand transmissions per each $\mathcal{SF}$ and the packet reception ratio (PRR) measurements are taken for each ED node at the GW node as seen in Fig. 14(b). Node A leverages a PRR greater than 95% for all $\mathcal{SF}$s due to its direct link communication with GW. In the other side, node B has a PRR less than 20% for $\mathcal{SF} = 7, 8$ and more than 90% for other $\mathcal{SF}$s, mainly due to blockage induced by the campus buildings. In addition, node C is attached with

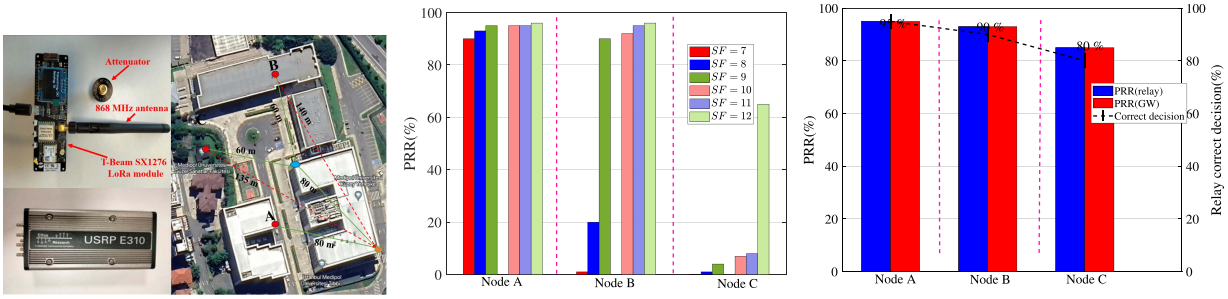

Fig. 14. Experimental setup. (a) Test equipment and location. (b) PRR without relay at different nodes. (c) PRR with the proposed relay at different nodes.

a 30-dB attenuator to simulate harsh environment scenarios, resulting only in a reliable communication with $\mathcal{SF} = 12$ at PRR level greater than 60%.

In the second part of the experiment, the relay is incorporated in the network to test its ability to schedule the transmitting nodes. Fig. 14(c) illustrates the PRR at the relay for the three nodes (blue). Both node A and node B ensure more than 90% PRR and since the relay can detect signal it successfully forwards it to the GW. For the scheduling process the relay holds whenever it receives the node A signal. But for node B it alters it transmission $\mathcal{SF}$ to 9. For node C, the relay is only able to reliably receive its signal at $SF = 9$ where it schedules it to change its $\mathcal{SF}$ to 12. The obtained results in this part of experiment directly aligns with the obtained results in the first part.

VII. Conclusion

This article presented the design, implementation, and performance examination of a novel decentralized dynamic relaying mechanism for LoRaWAN is proposed, which integrates harmoniously with the constraints of the existing specifications. The network-invisible smart relay obviates the need for adjustments to network topology or standards, allowing smooth incorporation into industrial deployments. In order to optimize the success probability based on SNR/SIR, a positioning algorithm is developed to determine the most efficient placement for the relay. On top of that, the coverage area is divided into EAB-SF discs, and the dynamic allocation of TxParams is determined by the observed success probabilities at each communication phase. Through this adaptive relaying mechanism, the data rate and coverage area are substantially improved. Furthermore, an FC shuffling mechanism is proposed to mitigate the limitations arising from collisions, while minimizing the complexity of the overall relaying block. The experimental results indicate that the proposed mechanism achieves a remarkable 40% extension in coverage area and success probability, along with a 50% increase in throughput due to ToA savings and collision reduction. Future research endeavors will explore novel techniques for adaptive sharing of different activation keys, catering to both over-the-air activation (OTAA) and authentication by personalization (ABP) mechanisms.

References

[1] K. Mekki, E. Bajic, F. Chaxel, and F. Meyer, "A comparative study of LPWAN technologies for large-scale IoT deployment," *ICT Exp.*, vol. 5, no. 1, pp. 1–7, 2019.

[2] W. Saad, M. Bennis, and M. Chen, "A vision of 6G wireless systems: Applications, trends, technologies, and open research problems," *IEEE Netw.*, vol. 34, no. 3, pp. 134–142, May/Jun. 2020.

[3] A. Augustin, J. Yi, T. Clausen, and W. M. Townsley, "A study of LoRa: Long range & low power networks for the Internet of Things," *Sensors*, vol. 16, no. 9, p. 1466, 2016.

[4] J. P. S. Sundaram, W. Du, and Z. Zhao, "A survey on LoRa networking: Research problems, current solutions, and open issues," *IEEE Commun. Surveys Tuts.*, vol. 22, no. 1, pp. 371–388, 1st Quart., 2020.

[5] L. Beltramelli, A. Mahmood, P. Österberg, and M. Gidlund, "LoRa beyond ALOHA: An investigation of alternative random access protocols," *IEEE Trans. Ind. Informat.*, vol. 17, no. 5, pp. 3544–3554, May 2021.

[6] (LoRa Alliance, San Ramon, CA, USA). *TS001-1.0.4 LoRaWAN® L2 1.0.4 Specification*. (2020). [Online]. Available: https://lora-alliance.org/wp-content/uploads/2021/11/LoRaWAN-Link-Layer-Specification-v1.0.4.pdf

[7] L. Vangelista, "Frequency shift chirp modulation: The LoRa modulation," *IEEE Signal Process. Lett.*, vol. 24, no. 12, pp. 1818–1821, Dec. 2017.

[8] O. Georgiou and U. Raza, "Low power wide area network analysis: Can LoRa scale?" *IEEE Wireless Commun. Lett.*, vol. 6, no. 2, pp. 162–165, Apr. 2017.

[9] U. Noreen, A. Bounceur, and L. Clavier, "A study of LoRa low power and wide area network technology," in *Proc. Int. Conf. Adv. Technol. Signal Image Process. (ATSIP)*, 2017, pp. 1–6.

[10] (LoRa Alliance, San Ramon, CA, USA). *RP002-1.0.4 Regional Parameters*. (2022). [Online]. Available: https://resources.lora-alliance.org/technical-specifications/rp002-1-0-4-regional-parameters

[11] J. Petajajarvi, K. Mikhaylov, A. Roivainen, T. Hanninen, and M. Pettissalo, "On the coverage of LPWANs: Range evaluation and channel attenuation model for LoRa technology," in *Proc. 14th Int. Conf. its Telecommun. (ITST)*, 2015, pp. 55–59.

[12] H. P. Tran, W.-S. Jung, D.-S. Yoo, and H. Oh, "Design and implementation of a multi-hop real-time LoRa protocol for dynamic LoRa networks," *Sensors*, vol. 22, no. 9, p. 3518, 2022.

[13] P. J. Radcliffe, K. G. Chavez, P. Beckett, J. Spangaro, and C. Jakob, "Usability of LoRaWAN technology in a central business district," in *Proc. IEEE 85th Veh. Technol. Conf. (VTC)*, 2017, pp. 1–5.

[14] "3rd generation partnership project; technical specification group radio access network; study on NR network-controlled repeaters; (Release 18)," 3GPP, Sophia Antipolis, France, Rep. 38.867, 2022.

[15] M. Lauridsen, B. Vejlgaard, I. Z. Kovacs, H. Nguyen, and P. Mogensen, "Interference measurements in the European 868 MHz ISM band with focus on LoRa and SigFox," in *Proc. IEEE Wireless Commun. Netw. Conf. (WCNC)*, 2017, pp. 1–6.

[16] W. Xu, G. Cai, Y. Fang, S. Mumtaz, and G. Chen, "Performance analysis and resource allocation for a relaying LoRa system considering random nodal distances," *IEEE Trans. Commun.*, vol. 70, no. 3, pp. 1638–1652, Mar. 2022.

[17] (LoRa Alliance, San Ramon, CA, USA). *LoRaWAN® Relay Specification TS011-1.0.0*. (2022). [Online]. Available: https://resources.lora-alliance.org/technical-specifications/ts011-1-0-0-relay

[18] M. R. Islam, M. Bokhtiar-Al-Zami, B. Paul, R. Palit, J.-C. Grégoire, and S. Islam, "Performance evaluation of multi-hop LoRaWAN," *IEEE Access*, vol. 11, pp. 50929–50945, 2023.
[19] J. Haxhibeqiri, I. Moerman, and J. Hoebeke, "Low overhead scheduling of LoRa transmissions for improved scalability," *IEEE Internet Things J.*, vol. 6, no. 2, pp. 3097–3109, Apr. 2019.
[20] B. Reynders, Q. Wang, P. Tuset-Peiro, X. Vilajosana, and S. Pollin, "Improving reliability and scalability of LoRaWANs through lightweight scheduling," *IEEE Internet Things J.*, vol. 5, no. 3, pp. 1830–1842, Jun. 2018.
[21] D. Lundell, A. Hedberg, C. Nyberg, and E. Fitzgerald, "A routing protocol for LoRa mesh networks," in *Proc. IEEE 19th Int. Symp, World Wireless, Mobile Multimedia Netw. (WoWMoM)*, 2018, pp. 14–19.
[22] G. Zhu, C.-H. Liao, T. Sakdejayont, I.-W. Lai, Y. Narusue, and H. Morikawa, "Improving the capacity of a mesh LoRa network by spreading-factor-based network clustering," *IEEE Access*, vol. 7, pp. 21584–21596, 2019.
[23] H.-C. Lee and K.-H. Ke, "Monitoring of large-area IoT sensors using a LoRa wireless mesh network system: Design and evaluation," *IEEE Trans. Instrum. Meas.*, vol. 67, no. 9, pp. 2177–2187, Sep. 2018.
[24] M. Jouhari, N. Saeed, M.-S. Alouini, and E. M. Amhoud, "A survey on scalable LoRaWAN for massive IoT: Recent advances, potentials, and challenges," *IEEE Commun. Surveys Tuts.*, vol. 25, no. 3, pp. 1841–1876, 3rd Quart., 2023.
[25] D. Mugerwa, Y. Nam, H. Choi, Y. Shin, and E. Lee, "SF-partition-based clustering and relaying scheme for resolving near–far unfairness in IoT multihop LoRa networks," *Sensors*, vol. 22, no. 23, p. 9332, 2022.
[26] P. Tian, C. A. Boano, X. Ma, and J. Wei, "LoRaHop: Multi-hop support for LoRaWAN uplink and downlink messaging," *IEEE Internet Things J.*, vol. 10, no. 17, pp. 15376–15392, Sep. 2023.
[27] D. Mugerwa, Y. Nam, H. Choi, Y. Shin, and E. Lee, "Implicit overhearing node-based multi-hop communication scheme in IoT LoRa networks," *Sensors*, vol. 23, no. 8, p. 3874, 2023.
[28] S. Lee, J. Lee, H.-S. Park, and J. K. Choi, "A novel fair and scalable relay control scheme for Internet of Things in LoRa-based low-power wide-area networks," *IEEE Internet Things J.*, vol. 8, no. 7, pp. 5985–6001, Apr. 2021.
[29] Z. Sun, H. Yang, K. Liu, Z. Yin, Z. Li, and W. Xu, "Recent advances in LoRa: A comprehensive survey," *ACM Trans. Sens. Netw.*, vol. 18, no. 4, pp. 1–44, 2022.
[30] J.-T. Lim and Y. Han, "Spreading factor allocation for massive connectivity in LoRa systems," *IEEE Commun. Lett.*, vol. 22, no. 4, pp. 800–803, Apr. 2018.
[31] A. Mahmood, E. Sisinni, L. Guntupalli, R. Rondón, S. A. Hassan, and M. Gidlund, "Scalability analysis of a LoRa network under imperfect orthogonality," *IEEE Trans. Ind. Informat.*, vol. 15, no. 3, pp. 1425–1436, Mar. 2019.
[32] O. Dieng, C. Pham, and O. Thiare, "Comparing and adapting propagation models for LoRa networks," in *Proc. 16th Int. Conf. Wireless Mobile Comput., Netw. Commun. (WiMob)*, 2020, pp. 1–7.
[33] "Electromagnetic compatibility and radio spectrum matters (ERM); short range devices (SRD); radio equipment to be used in the 25 MHz to 1 000 MHz frequency range with power levels ranging up to 500 mW; part 1: Technical characteristics and test methods; Version 3.1.1," ETSI Sophia Antipolis, France, Rep. EN 300 220-1, Feb. 2017. [Online]. Available: https://www.etsi.org/deliver/etsi_en/300200_300299/30022001/03.01.01_60/en_30022001v030101p.pdf
[34] J. Lyu, D. Yu, and L. Fu, "Analysis and optimization for large-scale LoRa networks: Throughput fairness and scalability," *IEEE Internet Things J.*, vol. 9, no. 12, pp. 9574–9590, Jun. 2022.
[35] D. Croce, M. Gucciardo, S. Mangione, G. Santaromita, and I. Tinnirello, "Impact of LoRa imperfect orthogonality: Analysis of link-level performance," *IEEE Commun. Lett.*, vol. 22, no. 4, pp. 796–799, Apr. 2018.
[36] K. Ronasi, V. S. W. Wong, and S. Gopalakrishnan, "Distributed scheduling in multihop wireless networks with maxmin fairness provisioning," *IEEE Trans. Wireless Commun.*, vol. 11, no. 5, pp. 1753–1763, May 2012.
[37] K. Deb, *Multi-Objective Optimization Using Evolutionary Algorithms*, vol. 16, Hoboken, NJ, USA: Wiley, 2001.
[38] F. Benkhelifa, Y. Bouazizi, and J. A. McCann, "How orthogonal is LoRa modulation?" *IEEE Internet Things J.*, vol. 9, no. 20, pp. 19928–19944, Oct. 2022.
[39] K. Deb, A. Pratap, S. Agarwal, and T. Meyarivan, "A fast and elitist multiobjective genetic algorithm: NSGA-II," *IEEE Trans. Evol. Comput.*, vol. 6, no. 2, pp. 182–197, Apr. 2002.
[40] A. Waret, M. Kaneko, A. Guitton, and N. El Rachkidy, "LoRa throughput analysis with imperfect spreading factor orthogonality," *IEEE Wireless Commun. Lett.*, vol. 8, no. 2, pp. 408–411, Apr. 2019.

Hamza Haif (Graduate Student Member, IEEE) received the B.E. and M.Sc. degrees in electrical engineering from the Institute of Electrical and Electronic Engineering, University of M'Hamed Bougara Boumerdes, Boumerdes, Algeria, in 2019 and 2022, respectively. He is currently pursuing the Ph.D. degree with the Communications, Signal Processing, and Networking Center (CoSiNC), Istanbul Medipol University, Istanbul, Turkey.

He is also a member of the CoSiNC, Istanbul Medipol University. His research focuses on 5G and beyond radio access technologies, waveform design, joint radar (sensing) and communication designs, Internet of Things, and wide-area networks.

Abdelali Arous (Graduate Student Member, IEEE) received the B.E. and M.Sc. degrees in electrical engineering from the Institute of Electrical and Electronic Engineering, University of M'Hamed Bougara Boumerdes, Boumerdes, Algeria, in 2019 and 2022, respectively. He is currently pursuing the Ph.D. degree with the Communications, Signal Processing, and Networking Center (CoSiNC), Istanbul Medipol University, Istanbul, Turkey.

He is also a member of the CoSiNC, Istanbul Medipol University. His research focuses on 5G and beyond radio access technologies, waveform design, joint radar (sensing) and communication designs, Internet of Things, and wide-area networks.

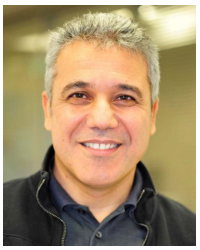

Hüseyin Arslan (Fellow, IEEE) received the B.S. degree from Middle East Technical University, Ankara, Turkey, in 1992, and the M.S. and Ph.D. degrees from Southern Methodist University, Dallas, TX, USA, in 1994 and 1998, respectively.

From January 1998 to August 2002, he was with the Research Group of Ericsson, Morrisville, NC, USA, where he was involved with several projects related to 2G and 3G wireless communication systems. Since August 2002, he has been with the Electrical Engineering Department, University of South Florida, Tampa, FL, USA, where he is a Professor. In December 2013, he joined Istanbul Medipol University, Istanbul, Turkey, to found the Engineering College, where he has worked as the Dean of the School of Engineering and Natural Sciences. In addition, he has worked as a part-time Consultant for various companies and institutions, including Anritsu Company, Morgan Hill, CA, USA, and The Scientific and Technological Research Council of Turkey, Ankara. He conducts research in wireless systems, with emphasis on the physical and medium access layers of communications. He has been collaborating extensively with key national and international industrial partners and his research has generated significant interest in companies, such as InterDigital, Anritsu, NTT DoCoMo, Raytheon, Honeywell, and Keysight technologies. Collaborations and feedback from industry partners have significantly influenced his research. In addition to his research activities, he has also contributed to wireless communication education. He has integrated the outcomes of his research into education which lead him to develop a number of courses at the University of South Florida. He has developed a unique "Wireless Systems Laboratory" course (funded by the National Science Foundation and Keysight technologies) where he was able to teach not only the theory but also the practical aspects of wireless communication system with the most contemporary test and measurement equipment. His current research interests are on 5G and beyond radio access technologies, physical-layer security, interference management (avoidance, awareness, and cancellation), cognitive radio, multicarrier wireless technologies (beyond OFDM), dynamic spectrum access, co-existence issues, nonterrestial communications (high-altitude platforms), and joint radar (sensing) and communication designs.

Dr. Arslan has served as the general chair, technical program committee chair, session and symposium organizer, workshop chair, and technical program committee member in several IEEE conferences. He is currently a member of the editorial board for the IEEE COMMUNICATIONS SURVEYS AND TUTORIALS and the *Sensors*. He has also served as a member of the editorial board for the IEEE TRANSACTIONS ON COMMUNICATIONS, the IEEE TRANSACTIONS ON COGNITIVE COMMUNICATIONS AND NETWORKING, and several other scholarly journals by Elsevier, Hindawi, and Wiley Publishing. He is a Fellow of NAI and an IEEE Distinguished Lecturer.